REPORT DOCUMENTATION PAGE

Form Approved OMB No. 0704-0188

1. AGENCY USE ONLY (Leave blank)	2. REPORT DATE	3. REPORT TYPE AND DATES COVERED
	1995	Final Report

4. TITLE AND SUBTITLE

Study of Relationship Between Coronal Mass Ejections and the Electron Component of Solar Energetic Particles

5. FUNDING NUMBERS

F6170894W0902

6. AUTHOR(S)

Dr. Vladislav G. Stolpovskii

7. PERFORMING ORGANIZATION NAME(S) AND ADDRESS(ES)

Institute for Nuclear Physics
Moscow 119899
Russia

8. PERFORMING ORGANIZATION REPORT NUMBER

N/A

9. SPONSORING/MONITORING AGENCY NAME(S) AND ADDRESS(ES)

EOARD
PSC 802 BOX 14
FPO 09499-0200

10. SPONSORING/MONITORING AGENCY REPORT NUMBER

SPC 94-4071

11. SUPPLEMENTARY NOTES

12a. DISTRIBUTION/AVAILABILITY STATEMENT

Approved for public release; distribution is unlimited.

12b. DISTRIBUTION CODE

A

13. ABSTRACT (Maximum 200 words)

This report results from a contract tasking Institute for Nuclear Physics as follows: Investigate the separation of the effects of coronal transport and acceleration on open magnetic field lines, develop a model of the role of CME's in acceleration and escape of nonrelativistic and relativisic electrons.

14. SUBJECT TERMS

EOARD

15. NUMBER OF PAGES

26

16. PRICE CODE

N/A

17. SECURITY CLASSIFICATION OF REPORT	18. SECURITY CLASSIFICATION OF THIS PAGE	19. SECURITY CLASSIFICATION OF ABSTRACT	20. LIMITATION OF ABSTRACT
UNCLASSIFIED	UNCLASSIFIED	UNCLASSIFIED	UL

FINAL REPORT
to contract SPC-94-4071 EOARD/AFMC.

Title of Project: "Study of relationship between coronal mass ejections and the electron component of solar energetic particles".

Contractors: V.G.Stolpovskii and E.I.Daibog (both Nuclear Physics Institute of Moscow State University, 119899 Moscow, Vorobjevy Gory, Russia).

The contract SPC-94-4071 was accomplished from October 1994 to October 1995. In the framework of the contract it was necessary - to separate the effects of coronal transport and acceleration on open magnetic field lines and to estimate the azimuthal spread of particles following the solar flare; - to develop understanding of the role of coronal mass ejection (CME) in acceleration and escape of nonrelativistic and relativistic electrons; - to determine the efficiency of interplanetary shocks for acceleration of different particles speices, including electrons in wide energy range . These topics are presented in the Final Report which consists of following parts:

1. Introduction.
2. Data sources and event selection.
3. Research methods and normalization procedures.
4. Geometric consideration of CME locations and velocities.
5. Helios and ISSE 3 data and results.
6. Phobos data and results.
7. Conclusions.
Acknowledgements.
References.

1. Introduction.

There are a lot of serious questions on Solar Energetic Particle (SEP) events. One of them is: whether SEPs in interplanetary space are flare or CME (Coronal Mass Ejection)-driven shocks associated.

Different scenarios of activities accompaning SEP events exist. One of possible qualitative pictures is that at least those particles which eventually escape into space are accelerated by a coronal shocks produced by the flare or in some dynamical process which causes both flare impulsive phase and coronal shock. According to this picture a flare begins with rapid relaxation of unstable magnetic field configuration. Magnetic field relaxation and/or annihilation and reconnection accelerate the bulk coronal plasma and heat 10-100 keV electrons and ions predominantly. Electrons emit impulsive hard X-rays (Xh) via bremsstrahlung and impulsive microwave (cm) bursts via gyrosinchrotron (or plasma) emission. Those electrons which escape along open field lines excite type III radio emission. Rapid heating and/or mass ejection generates shock wave which spread out through large portion of the corona at speeds up to 2000 km/s [Lin and Hudson,1974; Cliver et al,1983]. The shock can further accelerate ambient energetic particles produced in the impulsive phase. While the shock is sufficiently strong it can continuously and selectively "extract" electrons and ions from shock-processed plasma along its evolving front and accelerate electrons up to 1-10 MeV and ions up to 0.1-1 GeV/nucl [Lee,1982; lee and Ryan,1986]. In this case a substantial number of accelerated particles escape into space.→

At high altitudes shock-accelerated electrons produce metric type-IY emission via the synchotron process and flare continuum radio emission. At low altitudes accelerated electrons generate cm-emission and Xh- and gamma rays as they interact with denser regions of the corona and chromosphere. Accelerated ions at low altitudes produce neutrons and gamma line emission through nuclear interactions. Their radiation signatures do not generally correlate well to those of particles higher in the corona or in interplanetary space. Though some of these contradictions were explained in [Daibog et al,1988] considering high and low coronal trapping the problem is still unresolved.

The model pictures developed in eighties is more problematic now especially as for paradigm of causality of flares and coronal mass ejections (CME) [Kahler,1991; Gosling,1993]. In any case if particles were accelerated at shocks it`s necessary to select them on intensity-time profiles of SEP events.

As a whole particle acceleration by shocks is widespread phenomenon in the heliosphere and many astrophysical objects [Axford,1981; Blandford,1994]. In the case of solar flares (or CME-driven shocks) we have so called travelling shocks. Although it was recognized in the late sixties [Rao,1967] that particle enhancements associated to shocks are due to an acceleration in interplanetary space and not to trapping of particles accelerated at flare as first suggested, it has only recently been recognized that shocks are of fundamental importance for SEP events [Evenson et al,1982; Cane et al, 1988].

At first it was a belief that the effect of a shock is limited to a local enhancement at shock passage, supperimposed on the decay phase of SEP event. In such a picture the shock locally accelerates some of solar particles. Later it was argued [Cane et al,1988] that almost complete profile of SEP events at 1 AU could be understood in terms of the large-scale structure of shock and connection of observation point with shock along magnetic field lines. CME-driven shocks typically have angular extents of about 50 deg. [Cane et al,1988], but for very energetic CMEs this extent is much more and the largest coronal and interplanetary shocks cover of about 180 deg [Kallenrode et al,1993; Cliver et al,1995]. However, there is an asymmetry with the eastern shock flank being more effective for acceleration than western one.

An important result from the study of the radio emisson is that the fastest shocks decelerate considerably in transit to the Earth and that these are flare associated. Slower shocks which are associated with erupting filaments tend to travel with more uniform speeds.

There is widespread opinion that eastern events are only observed if there is an interplanetary shock [Cane,1995]. Futheremore intensity-time profiles of SEP events are well organized by the solar longitude of associated flares and in terms of shock structure and transit speeds of the individual shocks. To understand the particle profiles it`s important to note that particles are restrained to flow along field lines. An observer at the Earth is connected to a position on the Sun of ~W60. It seems that shocks are rarely detected from such a location. Moreover according to this opinion the majority of western event shocks are either not seen or have minimal effects. For these events the profiles at all energies have a prompt onset with a rapid rise to maximum intensity followed by exponential decay. Such profiles can result from short injection at the Sun followed by diffusion in interplanetary space. A short injection time can be explained by the observer being connected to a strong shock for only a short time. For events originating futher East than ~E20 shocks are→

clearly of crucial importance since such events are always associated with shocks. For all events with a shock the particle intensity-time profile as a function of energy depends on the strength of the shock which is gauged by the transit speed.

The maximum energy at which there is a clear shock effect is dependent on the shock velocity. However, for the vast majority of events east of about W10 even if there is not a clear shock effect, only at energies about 50 MeV do the profiles look "diffusive".

One tends to interpret these sequences of profiles in terms of a solar component and an interplanetary one. In terms of continious acceleration at a single shock two components can be regarded as particles accelerated close to the Sun and those ones accelerated in the vicinity of observer which have not yet propagated away from the shock. It is clear that for western events one observes high intensity promptly because of connection to the strongest part of the shock when it is in the low corona. One expects the acceleration efficiency to be greatest near the Sun where shocks are fastest and the ambient plasma is dense. Futheremore, the conditions are more favorable for wave production because of high particle density. With time the field lines on which the observer is located connect more to flanks of the shock where acceleration is probably less efficient. Possibly more important is that the observer is connected to a shock that is higher in the corona. Lee and Ryan [Lee and Ryan,1986] considered analytically time-dependent coronal shock acceleration supposing cold plasma mass density ahead of the shock decreases as 1/r**2 and following diffusion coefficient k & r**2/t. It means strong acceleration near the Sun but this is in disagreement with Helios observations of scattering conditions [Kallenrode,1993]. The model [Lee and Ryan,1986] permits to accelerate protons from the initial energy of about 0.5 MeV to very high energy at the maximum of shock accelerated population. Proton energy reachs the value of 10 MeV and 1 GeV during tens of seconds and tens of minutes, respectively.

Another theoretical investigation by Ellison and Ramaty [Ellison and Ramaty,1985] has shown that electron, proton and alpha-particle spectra can be fitted well above 100 keV for electrons and 1 MeV/nucl for nuclei by assuming planar stationary shock acceleration with exponential cutoff in energy due to finite spatial extent of the shock. And the good fit is accomlished with the same shock compression ratio for all species. The model predicts that acceleration time to a given energy will be approximately equal for electrons and protons and, for reasonable parametrs in acceleration region can be on the order of magnitude of some seconds at ~100 MeV. There are other theoretical models (for example, [Krymsky and Petuchov,1980; Prischep and Ptuskin,1981]) in the framework of which it could be possible to accelerate electrons and ions to high energy.

So we can summarise: the theory predicts that shocks principally could accelerate electrons and ions to rather high energy, but every model has very special and strong suppositions and limits.

As for observations of shock accelerated particles there are clear evidencies and identifications of shock particle enhancements at low energies (hundreds keV for protons and few keV for electrons). Tsurutani and Lin [1982] divide ion and electron flux variations associated with interplanetary shocks into four types, which can be understood in terms of different acceleration mechanisms:
1) a slow quasi-exponential rise beginning several hours before the passage of the shock with a nearly constant upstream anisotropy which drops suddenly with the arrival of the shock. The local shock geometry (quasi-parallel) together with the features→

of the particle event is in agreement with the predictions from diffusive shock mechanism [Blandford and Ostriker,1978];
2) a spike of a few minutes duration at or near quasi-perpendicular shock. These events can be understood in terms of shock-drift acceleration, where the particle gains energy due to gradB drift in the induced electric field in the shock front [Decker,1983];
3) Step-like post-shock increases are associated with enhaneced turbulence behind the shock. This turbulence leads to efficient acceleration as well as storage of energetic particles;
4) No significant variation at all. These "non-events" increase in number as one goes to higher energies indicating that despite the proven ability of a shock to accelerate particles, we should not necessarily expect particle acceleration at each shock. Non-events can be observed in connection with quas-parallel as well as quasi-perpendicular shocks.

In a correspondence to shock wave influence the classification of SEP-events with higher energy protons was done in [Cane et al,1990; Kallenrode and Wibberenz,1992]. On the basis of statistics of 348 events registered onboard Helios s/cs at 0.3-1.0 AU Kallenrode and Wibberenz [1992] distinguished three types of shock influence on >10 MeV proton intensity profiles:
1) shocks leading to no increase in proton intensity (46%);
2) shock leading to rising and decaying intensity profile with maximum near the time of shock passage (22%) or to steplike postshock increase (2%);
3) "classical ESP-event when an intensity-time profile consists of prompt and shock-accelerated components(30).
A comparison of these protons with helium of the same energy/nucleon range gives the following conclusion; if there is no proton increase, there is also no increase in helium. The opposite is not true: sometimes there are shock-related proton increase, but there are no icrease in helium.

Cane et al. [1990] divided particle events associated with CME/ shock pairs into four groups according to relative intensities of prompt and shock-accelerated components for protons with >4 MeV energy. Group 1 contains events which have strong prompt and shock components are associated with high-velocity CMEs originating near central meridian flares (relative to an observer). Group 2 consists of events which have strong prompt and weaker shock components and are associated with western hemisphere flares and high velocity CMEs. Group 3 consists of events with absent prompt and large shock components; CMEs probably originate near central meridian and have velocity in the range <500-600 km/s. Group 4 events show no particle enhancements and are related to slow CMEs and slow shocks. In this study the conclusion about shock effect dependence on the connection longitude of an observation point was supported [Cane et al.,1988]

However it`s not clear how can we apply the above schemes to more energetic electrons (E>0.1 MeV). The main difference with low energies is that energetic electrons are much faster particles and can more easily escape from the shock front and their motion has another time as well as lenth scales. Moreover they can go away and greatly outstrip a shock front. This can considerably distort classical diffusion accelerated particle profile.

The majority of observations both at low and high energies concerns interplanetary protons. As for electrons direct observations of interplanetary electron fluxes are far less numerous. That is why indirect methods using radio and X-ray measurements are employed in a case of electrons. Unfortunately application of these measurements are extremely model-dependent.

Surely direct measurements of electrons in space are preferable as compared to any secondary effects caused by accelerated electrons. Such measurements are not numerous and unambiguos. There are both pro and contra arguments for shock relativistic electron acceleration. The character of flux time profiles in many impulsive electron events (delta function injection [Kallenrode and Wibberenz,1991], no evidence for more than one injection phase [Lin et al,1982]), nearly the same value of escape efficiency in flares of different power [Lin and Hudson,1971; Daibog et al,1989], similarity of the size distributions of the peak intensities of >70 keV electrons and >55 keV X-ray [Daibog et al,1989], similarity of the spectra shape for both small and large events [Lin,1985] and so on could be considered as evidencies of nearly exclusively impulsive relativistic and mild relativistic electron acceleration.

On the other hand observations of streams of electrons lasting for many hours following large flares [Lin,1985], electron events without hard X-ray assosiation [Daibog et al,1989] and other arguments (see [Kahler et al,1994]) can be supports of the opposite point of view, i.e. these electrons must be a result of extended acceleration and a shock source is a possible explanation for these events. Thus up to now the contribution to the interplanetary electron fluxes from acceleration in coronal or interplanetary shocks is poorly understood.

In our previous paper [Kahler et al,1994] we studied shock acceleration of nonrelativistic electrons. If these electrons in SEP events can arise from either flares or shocks, then we should expect that the escape efficiency (a ratio of peak electron flux to Xh-ray fluence) should be smaller for flares not accompanied by coronal shocks than for shock associated flares. We found only small difference between escape efficiencies of >70 keV electrons for groups of CME associated and non-associated flares. It could be considered that the shock population is no greater than that of the impulsive component. But statistics was not rich enough and we took into account only well-connected events, so the conclusion must be cleared up.

2. Data sources and event selection.

Data bank for this project includes an information on SEP-events, flares, CMEs and interplanetary conditions. The source of energetic particle data was experiments on Helios, ISEE 3, Phobos and also our measurements on Prognoz and Venera s/c for the periods of 1979-1982 and 1988-1989, i.e. near maxima of 21st and 22nd solar activity cycles when many flares and CMEs occured. In the case of "another`s" measurements we processed the information on fluxes, spectra and anisotropy of energetic particles which was given us for earlier investigations (e.g., see [Kallenrode et al,1991]). In addition, some events from the periods considered are described in literature [Cane et al,1988,1990; Moses and Evenson,1989; Beeck et al,1990; Mardsen et al,1991; Kallenrode,1993a,b; Kallenrode et al,1991,1992,1993; Daibog et al,1993; Kahler et al,1994; Logachev et al,1995] and we used the results of these publications.

Helios s/c were in a highly eccentric orbits around the Sun with radial distances between 0.3 and 1.0 AU. Semiconductor telescope measured electrons between 0.3 and 3 MeV in three energy channels and protons and nuclei with energy from 4 to 50 MeV/nucl in some differential channels and >50 MeV/nucl. Time resolution of measurements was ~3 min. The revolution of s/c around the axis perpendicular to the ecliptic plane provided data about the angular distribution of electrons and protons.→

The ISEE 3 s/c was in the inner Lagrangian point between Sun and the Earth. Electrons with energy between 0.22 and 2.0 MeV and 4 - 19 MeV were measured in the GSFC medium-energy cosmic ray experiment. Time resolution of electron measurements was high enough and we used 15 min averaged data in our investigation in according to [Richardson,1994]

In the case of Phobos electrons with energy between 0.35 and 1.5 MeV were registered during the cruise phase and the Martian orbit phase, i.e. at radial distances between 1.0 and 1.5 AU with time resolution ~ 20 min. The LET instrument was four-element n-p telescope which was able to measure protons and nuclei with energy of MeVs - some tens MeV per nucl. too. For protons and alphas time resolution was four minutes and data about flux anisotropy could be obtained.

As for our measurements onboard Venera they were accomplished as s/cs follow a trajectory oscillating between Earth and Venus, i.e. 1.0 and 0.7 AU. Electrons with energy between 0.07 and 1.5 MeV and protons with energy between 1 and 230 MeV, both in four intervals were measured with time resolution of 10 min.

Standard information about Ha-flares and bursts of flare Xt- and radioemission was taken from Solar-Geophysical Data and from Internet network. In the case of electromagnetic bursts we used not only table data but also intensity-time plots. An informatiom on corresponding Xh-bursts was provided by HXRBS observations on SMM [Dennis et al,1991a,b; 1992a,b]. Moreover, amplitude, spectral and time characteristics of Xh-bursts were obtained by means of X-ray detectors on Venera s/cs.

During the periods considered CMEs were observed by the Solwind coronagraph on P78-1 s/c at distance from 2.5Rs to 10Rs [Howard et al,1985] and coronagraph/polarimeter on SMM [Hundhausen et al,1984]. Data of Solwind observations were prepared by N.R.Sheeley from NRL and we obtained them from S.Kahler who made detailed comments to events selected. In the case of SMM observations we have a revised and expanded catalogue [Burkepile and St.Cyr,1993] which permits us to obtain time, velocity, position angle and other parameters of CMEs associated with selected SEP-events.

A relation between CMEs and interplanetary shocks in the time period of Helios observation was discussed in [Sheeley et al,1985, Cane et al,1988,1990]. For simultaneous observations of Helios and Venera we had data about interplanetary magnetic field (IMF) intensity vs. time and estimated some shock parameters directly. In the case of Phobos we had information on solar wind and IMF [Roatsch et al,1989] and use it for identification of interplanetary disturbancies.

Selection of electron events was made on the basis of >0.3 MeV electron intensity-time variations. Sharp intensity rise, followed by more or less gradual decay of the electron flux was considered as SEP-event. Those enhancements having duration more than 3 hours and amplitude exeeeding the background by 3 sigma were taken into account. It`s clear that background level depends on time and an observation point location and is different in various experiments considered here. But in any case we could distinguish electron enhancements with the amplitude of >0.3 MeV electron flux greater than 0.1 particle/sq.cm s sr.

The particle source identifications for the majority of large SEP-events which occurred during the time periods considered have been published previously (see [Cane et al,1988,1990; Kallenrode et al,1991; Daibog et al,1991,1993; Mardsen et al,1991]. We began, however, by making flare/CME associations without reference to these

previous studies. All the more that these studies were related to so-called proton events. We used usual method of the identification of parent flare (see, for example, [Van Hollebecke et al,1975]) and looked at the time correlation of the flare onset and the first arrival of energetic electrons to the observation point. The magnetic footpoint of the observation point was determined by the method described in [Notle and Roelof,1973], taking into account the real solar wind velocity. The associations derived were essentially the same as those arrived in earlier studies. The major difference of our event list is that it contains a number of smaller events which were not included in previous lists.

The angle between the location of the identified parent flare and the observer`s magnetic footpoint was in the limits 100W,E. The difference between the onset time of electron enhancements and that of the parent flare was in the interval of 10-100 min, which seems realistic, taking into account the value of that angle and radial distance of s/c and geometric factors of the detectors used.

3. Research methods and normalization prosedures.

There are some ways to develop an understanding of the relationship between electron component of SEP-events and CMEs and shocks. They propose an investigation of flux, spectrum and anistropy time behavior of energetic electrons in events related and not related to CMEs and its correlation with conditions at the Sun and in space. Our current investigation mainly concerns time profiles of SEP electron events associated to CME and flare.

We look for an evidence of CME-driven shock acceleration of electrons by examining rise times of subrelativistic electron events. We assume that if electron acceleration and injection is occuring during an extended period of shock propagation in the corona, the time intervals from event onset to maximum will be longer than in the case of impulsive acceleration. Also if shock acceleration is predominantly important comparing with impulsive phase injection this time interval will be longer than in the case of impulsive acceleration only. However if the major part of SEP event electrons is of a flare source and intensity time profile is defined by coronal and interplanetary diffusive propagation, the time interval under consideration is from onset of the flare to electron peak intensity time. So for all events we consider both these time intervals.

We suppose that there must be some correlation between rise time of SEP event profile and a speed of coronal shock. Indeed, as we know from the study of radio emission [Woo et al,1985; Cane et al,1986; Hundhaunsen et al,1994], fast CME speeds imply acceleration on going through corona followed by deceleration in transit to the Earth. Let us suppose for simplicity that CME speed is changing with constant acceleration "a" and CME driven shock can accelerate electrons if shock speed is higher than some Vlim. Let the CME speed rise till the value Vo. Then the time during which electrons should be shock accelerated increases with increasing Vo:

$$t = (Vo - Vlim)/a \qquad (1)$$

and a distance that shock travels during this time

$$S = (Vo^{**}2 - Vlim^{**}2)/2a \qquad (2)$$

also increase with increasing a speed Vo of CME. In a case of constant CME and shock speed Vo a distance at which shock can

accelerate particles, would be traveled by the shock in a time

$$t = S/Vo,$$

decreasing with increase of Vo. As a mattter of fact it is necessary to take into account damping of shock and decreasing of ambient plasma density. As a result formulae above could be considerably corrected, but as a whole the character of Vo vs t dependence would be the same: t(Vo) - decreasing function, if V = Vo = const, and t(Vo) - increasing function, if CME acceleration or deceleration takes place.

So as we know about acceleration - deceleration of the shock, we are waiting as a result of our investigation that rise time of SEP event is increasing function of CME traveling speed, because the injection continues for longer times with faster CMEs, and a size of injection region increases faster than linearly with CME speed.

We considered SEP-events which occurred at radial distance from 0.3 to 1.5 AU so it was necessary to normalize both onset and peak intensity times to the same distanance r=1 AU to exclude differences of time profiles due to propagation effects. The same procedure is of importance when comparing peak intensities of SEP events. Normalization of onset time is obvious. If the first particles were registered at the distance r1 on time t1, then they should be registered at the distance r2 on time t2=r2*t1/r1.

For recalculating peak times from one distance to another one it's necessary to employ some model notions. We used ideas of elementary diffusion model (for example, [Lin et al,1982]) and took into account a difference of angular distances between the observer`s magnetic footpoint and flare site. Here we used formalism of coronal propagation [Kunow et al,1991] which is supposed to be independent of the physical content of phenomena considered. So we used approximation formulae for coronal propagation of >0.5 MeV electrons from [Schellert et al,1985] and recalculated them for 0.3 MeV energy. A fit to the data was performed by assuming that the constant delay within certain angular distance phi0 (fast propagation region) is due to interplanetary propagation and that time to maximum tm increases linearly beyond phi0. The best fit was obtained for phi0 = 26 deg., and interplanetary propagation corresponding to mean free path lambda = 0.12 AU or below. The approximating formula for tm vs. phi is tm = -22 + 3.9 phi, min, phi >26 deg. If mean free path is independent of electron energy then for 0.3 MeV electrons we have

$$tm(1\ AU,phi)= 78 + 4.1(phi - 26),min,$$

where the first and the second terms describe interplanetary to r = 1 AU and coronal propagation, respectively. As our measurements were at different radial and angular distances it's necessary to normalize tm(r,phi) according to interplanetary part of this formula with unchanging coronal term. In case of diffusion time to maximum is

$$tm \& r**2/k,$$

where k is diffusion coefficient. We supposed k radially dependent in the form k & r**q, where q varied from 0 to 1.5 (proportionality coefficients are omitted, because they have no importance for normalization). Then recalculating tm from measured value at some distance r to 1 AU we have

$$tm(1\ AU) = tm*r**-(2-q).$$

So, normalized value of tm(r,phi) is

tmnorm ={tm(r,phi)-4.1(phi-26)}*r**-(2-q), (3)

where r in AU, phi in deg, t in min.

We consider two different variants for evaluation of SEP-event time parameters. The first is flare connected and we normalize time to maximum, i.e. time between maximum of electron enhancement and flare onset, tm(r,phi) and obtain tmnorm. The second one is dealing with elecrton rise time trise, i.e. time between onset and maximum of electron event. In this case we disregard coronal propagation. So

tnorm = t*r**-(2-q). (4)

We considered trise variant as controlling one.

Similarly for peak intensity Im we used phenomenological approximating formula from [Schellert et al,1985] for coronal attenuation:

Im & exp(-phi/23),

where phi in deg, and following interplanetary decreasing & r**-3. So

Imnorm = Im(r,phi)*exp(-phi/23)*r**3. (5)

4. Geometric consideration of CME locations and velocities.

Usually when describing CME - flare geometry, only apparent or projected onto the sky plane angles are used both for CME widths and positions of CME center. In [Hundhausen,1993] there were considered rigorous geometrical formulae though the author didn't use them in the data analysis and in particular in comparison of flare and apparent CME latitudes. Kahler et al [1989] calculated the solar position angle of the radial extension of the flare site when they studied spatial relationship between CMEs and flares, but their formula was not absolutely correct.

Our consideration is similar to Hundhausen`s one. We didn`t distinguish between solar equatorial and ecliptic planes. The rigorous formula for position angle of flare on the solar limb is

psi = arctg(tg teta x cos C/sin B), (6)

where teta and B are flare latitude and longitude, correspondingly, C is angle between solar rotation axis and sky plane. We know that maximum of C is about 7 deg., so we put cos C = 1. Using this formula we have obtained a plot of CME-flare position angles. It seems to us that it`s better to compare not flare latitudes but flare position angles to those of CME. We see
that for central flares the difference between flare latitude and flare position angle may be large and CME and flare position angles are closer to each other.

As we have some flares sited at the central meridian when a difference between true and apparent latitudes of CME can be significant, we used exact formulae for calculating true angular CME widths and speeds. For demonstration of the importance of these corrections we show the dependence of CME center position angle on position angle of flare and dependence of CME apparent latitude as a function of flare latitude. It follows from a comparison of these dependenses that the former is closer to linear dependence, so we don't dare to say that CMEs and flares are usually dramatically spaced and have no common reason. The result of this comparison is shown in fig. 1a,b.

It was necessary to restrict ourselves by definite geometrical model. We suppose that CME center coincides with the flare site and moves radially from the Sun and calculate CME angular widths and velocities. We assume also that velocity of CME-driven shock coincides with CME velocity.

If the cone containing CME intersects with limb plane then measured CME velocity is the real one. If not, - we obtain the "real" CME velocity by recalculation of the nearest to the sky plane forming of the CME cone. Recalculated Vcme is

$$Vcme = Vmeas/\cos(ksi-alpha/2), \qquad (7)$$

where ksi is an angle between radial flare extension and the sky plane,

$$ksi=\arccos[(costeta*sinB)^{**}2+(sinteta)^{**}2]^{**}1/2. \qquad (8)$$

Angle alpha in (7) is a real dimension of CME cone,

$$alpha=2arctg[(tgD/2)*cosksi], \qquad (9)$$

angle D is dimension of CME cone in sky plane from Sheeley`s list.

The time of arrival of CME-driven shock to the observer`s magnetic field line was obtained from an equations which takes into account angle between flare and observer`s magnetic footpoint, dimension of CME cone, solar wind velocity and CME speed. We solved numerically the next equation for determining this time:

$$\sin(alpha/2)/\{\cos(teta)*cosG\} - 1 = dzeta*Vsw/(R*omega), \qquad (10)$$

wbere G = dzeta +(-) (phi+45 deg - alpha/2), Vsw - solar wind speed at the observation point, phi is the difference between flare and s/c magnetic line footpoint longitudes, alpha is angular width of CME, R - solar radius, omega - solar angular rotation speed. "+" and "-" refer to western and eastern flares, respectively. dzeta is an angular distance between an intersection point of coronal shock and observer`s magnetic footpoint.
From obtained dzeta we can calculate a radial distance to intersection point and a time when CME-driven shock comes to observer`s magnetic field line.

We consider a shock expanding with CME speed and use following geometrical limits for CME shock-driven acceleration:
1. shock front is a hemisphere centred in a flare site;
2. shock front is a part of a sphere surface inside CME angular width cone.

In these two limits we estimated times of passage of shock across the field line connecting to observation point. These times are shown in Table 2 of the next paragpraph. We can compare them to observed SEP-event onset times. In the framework of geometry adopted it`s clear that when flare-CME is in FPR this time equals to 0. In the case of far western flares these times are too large and measured SEP-event onset times are incompatible with such consideration.

5. Helios and ISSE 3 data and results.

Data obtained in the case of Helios s/c observations are presented in tables 1,2 and 3. Parameters of flares and CMEs associated with selected SEP-events are shown in table 1.

Table 1.

Flares and CMEs associated to selected SEP-events.

1	2	3	4	5	6	7	8	9	10
					1979				
1.	03.04	0105	S25W14	0028	S88W(040)	S62W(020)	1000	1620	>9(>5)
2.	27.04	0639	N18E17	0640	N80E(080)	N48E(039)	690	1000	>20(>14)
3.	18.08	1345	N08E90	1345#	N40E(240)	N08E(240)	630#	630#	>49
4.	27.11	0647	N18E05	0724	N90(360)	N75(360)	600	600	##
					1980				
5.	02.03	1634	S28W71	1642	S45W(045)	S29W(043)	600	600	>32
6.	21.05	2049	S17W15	2045	S50W(100)	S44W(045)	400	590	##
7.	30.08	2026	S12E41	2046#	S45E(110)	S18E(060)	730#	1000#	###
8.	14.11	0730	W110	0710	N35W(090)	N35W(090)	1100	1100	5-30
					1981				
9.	25.01	0847	S12E90	0855	S30E(140)	S12E(140)	900	900	22-70
10.	11.04	1059	N11E53	1109	N25E(095)	N14E(083)	775	775	##
11.	08.05	2201	N09E37	2225	N20E(120)	N15E(094)	1000	1000	##
12.	10.05	1232	N10E90	1217	N20E(040)	N20E(040)	1420	1420	3-23
13.	13.05	0330	N10E55	0359	N25E(090)	N12E(079)	1500	1500	##
14.	16.05	0753	N11E14	0753#	N90(360)	N39(360)	600#	600#	>20
15.	04.06	1745	N20W16	1930	N80W(003)	N53W(003)	226	620	>52(>22)
16.	20.07	1310	S25W75	1320#	S30W(080)	S26W(069)	380#	380#	>67
17.	19.11	0245	W100	0220	N25W(050)	N25W(050)	800	800	##
18.	05.12	1432	N20W40	1324	N45W(060)	N30W(044)	840	920	>230
					1982				
19.	28.01	0630	N08E42	0642#	N30E(180)	N12E(180)	1000#	1480#	##
20.	31.01	2325	S14E13	2353	N85E(030)	N85E(009)	560	1600	7-21
21.	10.02	0104	N17E54	0104#	N40E(040)	N21E(034)	570#	600#	##
22.	02.06	1526	S08E81	1526#	N80W(130)	N80W(130)	550#	550#	##
23.	03.06	1142	S09E71	1136	N30E(040)	N30E(038)	1100	1100	##
24.	22.07	1630	N16W99	1702	N22W(090)	N16W(090)	1750	1750	##
25.	08.08	0204	S09W65	0224	S10W(010)	S10W(008)	600	640	18-200 (19-211)
26.	21.11	0605	S12W81	0600	S20W(060)	S12W(060)	735	735	##
27.	22.11	1740	S11W36	1740#	S10W(060)	S18W(040)	760#	910#	>27(>23)
28.	07.12	2340	S19W86	2335	S20W(100)	S10W(100)	1250	1250	##
29.	19.12	1541	N10W75	1541#	W(100)	W(098)	460#	460#	>22
30.	26.12	1040	S10E14	1940#	S20W(200)	S20W(118)	1700#	1700#	###
31.	03.02	0541	S17W07	0559	N90(360)	N90(360)	800	800	###

Here 1 is event number (this number will be remained in next table), 2 is event date, 3 - onset of Ha-flare,UT, 4 - flare location, 5 - CME limb time,UT, (# marks that we take it as flare onset time), 6 - observed position angle and angular width D (in parenthesisses) of CME,deg, 7 - corrected CME position angle and angular width alpha (in parenthesisses) calculated according to (9),deg, 8 - observed CME velocity Vmeas (# corresponds to an estimate of CME velocity when we take flare onset as limb time of CME),km/s, 9 - recalculated CME velocity Vcme according to (7),km/s (# corresponds to an estimate of CME velocity when we take flare onset as limb time of CME), 10 - time of intersection between CME-driven shock and observer's magnetic field line,min, obtained from (10) for shock propagation in a hemisphere and inside CME angular width cone (values in parenthesisses correspond to recalculated CME velocity Vcme, ## - to the observer's magnetic footpoint in FPR, ### - to the case when shock reaches observer's field line at very large distances and too late, respectively).

In table 2 time to maximum and risetime of >0.3 MeV electron intensity in selected Helios events are presented under different suggestions on coronal and interplanetary propagation.→

Table 2.

Time of intensity maximum in selected SEP-events

1	2	3	4	5	6	7	8	9	10	
1	0.75	S09E14	35	2.0	5.6	6.3	4.7	7.0	5.3	H1
	0.68	S07W08	19	1.5	4.3	6.1	4.1	6.9	4.7	H2
2	0.47	S07E16	19	>5.6	8.3	<5.9	<2.8	8.3	3.9	H1
3	0,99	N00W158	112	14.8	21.9	7.3	7.2	1.2	1.2	H1
	0.97	S05E159	70	14.1	17.7	6.4	6.2	0.6	0.6	H2
4	0.48	N05W02	15	7.1	9.2	8.5	4.1	11.5	5.5	H2
5	0.94	S06W17	58	16.8	20.5	4.0	3.8	1.8	1.7	H2
6	0.35	S05E02	19	21.3	23.3	16.8	5.8	22.2	7.7	H1
7	0.99	S00E171	131	21.9	6.3	8.6	8.5	2.9	2.8	
8	0.51	S07W134	24	8.0	12.1	15.5	8.0	17.5	9.0	
9	0.83	N04E30	62	9.2	21.0	17.3	14.4	10.6	8.8	
10	0.91	S03E48	15	11.6	13.1	1.8	1.6	2.7	2.5	
11	0.69	S08E57	25	22.8	0.7	4.0	2.7	5.8	4.0	
12	0.66	S06E69	26	15.5	23.0	17.2	11.4	16.7	11.0	
13	0.64	S06W69	22	4.3	8.5	9.5	6.1	11.1	7.1	
14	0.60	S07E58	47	8.5	9.5	2.8	1.7	0.6	0.4	
15	0.36	S06E28	51	19.7	2.2	15.9	5.7	12.6	4.5	
16	0.70	N05W139	71	13.8	17.6	7.9	5.5	2.9	2.0	
17	0.64	S06W108	8	2.5	3.8	2.7	1.7	3.0	1.9	
18	0.44	S07W135	95	16.2	23.0	35.0	15.4	18.4	8.1	
19	0.72	N05E63	21	7.4	9.0	3.5	4.3	4.8	3.5	
20	0.76	N05E57	51	0.3	3.8	6.1	4.6	4.7	3.6	
21	0.83	N04E55	13	1.4	3.1	2.5	2.1	2.9	2.4	
22	0.58	S07E73	8	15.6	16.8	3.4	2.0	3.9	2.3	
23	0.57	S07E73	3	12.4	13.2	2.8	1.6	4.4	2.5	
24	0.56	N07W91	9	17.8	20.0	7.1	4.0	11.1	6.2	
25	0.74	N05W108	45	2.8	9.2	11.8	8.7	13.0	9.6	
26	0.77	S05W97	17	6.7	7.5	1.2	0.9	2.3	1.8	
27	0.76	S05W96	60	19.0	22.4	5.9	4.5	4.9	3.7	
28	0.60	S07W99	18	23.8	1.8	5.6	3.4	5.9	3.5	
29	0.45	S07W116	44	16.0	17.2	5.9	2.7	4.2	1.9	
30	0.37	S06W126	140	11.1	13.2	15.5	5.7	1.7	0.6	
31	0.62	N06E90	100	7.0	12.0	16.0	10.0	3.3	2.0	

Here "1" is event number (the same as in table 1); "2" is radial distance to observation point,AU; "3" - heliographic latitude tetaob and longitude Bob of s/c`s magnetic footpoint; "4" is angular distance phi between observer`s magnetic footpoint and flare,deg; "5" is onset time of electron intensity increase tse, in hrs,UT; "6" is observed time of electron intensity maximum in hrs,UT; "7" is electron intensity rise time, hrs, normalized to radial distance r=1 AU with q=0 in accordance with (4); "8" is the same as"7" but with q=1; "9" is time to maximum tm normalized to FPR and 1 AU in accordance with (3) under q=0, hrs; "10" is the same as"9" but under q=1.

In Table 3 we show particle fluxes - measured and normalized to r=1AU and Fast Propagation region according to (5). For Jenorm we take into account coronal propagation according to angular distance between flare site and observer`s footpoint (column "phi"). "A"is a spacecraft -Sun-Earth angle.

Table 3.

Maximal fluxes of selected >0.3 MeV electron events

N	A	Jemeas	phi	Jenorm	Xt	typeII

1	E70	6.0E0	35(W)	4.2E0	M4	-	H1
	E28	3.0E2	FPR	9.4E1			H2
2	E48	1.1E2	FPR	1.0E1	X1	+	H1
3	W122	1.0E2	112(W)	3.9E3	X1	+	H1
	W151	1.5E3	70(W)	1.4E4			H2
4	E120	1.5E-1	96(W)	1.7E-1	C1	-	H1
	E30	2.5E1	FPR	2.6E0			H2
5	E80	3.0E-1	88(W)	5.6E0	M2	+	H1
	E30	8.0E0	58(W)	3.2E1			H2
6	E25	1.2E1	FPR	5.0E-1	X1	+	H1
7	W100	2.0E1		1.9E1	post limb		
8	W105	1.0E3	36(E)	3.1E2	M8	-	
9	E82	4.0E0	62(E)	1.1E1	M9	+	
10	E100	3.0E1	FPR	2.3E1	X1	+	
11	E95	8.0E3	FPR	2.6E3	M7	+	
12	E96	1.0E3	FPR	3.4E2	C4	-	
13	E94	9.0E2	FPR	2.4E2	X1	-	
14	E93	2.0E3	41(W)	1.1E3	X1	+	
15	E46	1.0E0	51(W)	1.3E-1	C3	+	
16	W90	2.0E2	71(E)	4.8E2	M5	+	
17	W80	5.0E2	FPR	1.3E2		+	
18	W80	8.0E0	100(E)	2.0E1	C3	-	
19	E98	7.0E2	FPR	2.6E2		+	
20	E97	4.0E2	51(W)	7.0E2		-	
21	E95	2.0E2	FPR	1.1E2	M3	+	
22	E105	2.0E1	FPR	4.9E0	X1	+	
23	E104	1.5E4	FPR	1.9E3	X8	+	
24	W65	2.0E3	FPR	3.5E2	M5	+	
25	W77	7.0E0	45(E)	8.1E0	M7	+	
26	W60	2.5E0	FPR	1.1E0	M1	-	
27	W61	1.5E1	63(E)	4.2E1	M7	+	
28	W86	1.2E4	FPR	2.6E3	X3	+	
29	W85	5.0E3	44(E)	1.1E3	M9	+	
30	W107	2.0E3	FPR	1.0E2	post limb		
31	E117	4.5E1	100(W)	3.1E2	X4	+	

Figs.2a and b show electron intensity rise time trise as a function of measured CME velocity for q=0 and q=1,respectively. Fig.3 is the same as fig.2, but for electron time to maximum tm. Fig.4 and 5 are the same as figs. 2 and 3, respectively, but for recalculated Vcme. We excluded from figs.4 and 5 points corresponding to events NN 20,22,23,30 and 31 from the list, for which flare and CME were in opposite hemispheres of the Sun, because the basic geometrical suppositions of coincidence of CME center and a flare site and radial remove of CME were not fulfilled for these events. On fig.4 and 5 open circles mark events observed at r < 0.4 AU (NN 6,15,18) because the using of diffusion approximation is doubtful at so small distances. In addition, we mark by open circles two more events (N 24 - post limb flare. N25 - far behind limb observer`s magnetic footpoint, intensity time profile shape of this event compels to suppose another flare optimally connected to observation point).
From figs.2-5 it may be seen that the more the CME velocity the more tm and trise, on average. In addition, a dispersion of points is less for propagation with q=1. This effect is more pronounced in the case of tm. Inspite of many uncertainties of fig.4 and 5 it`s possible to say about some correlation between corrected CME velocity and rise time and time to maximum. This correlation is larger in the case of tm.

ISEE data list consists of 24 events. These data were obtained at 1AU and consequently they are free of possible distortions connected with radial normalizing procedure. These results are presented in Tables 4 and 5

Table 4

Parent flares and CMEs of CEP events observed onboard ISEE 3

1	2	3	4	5	6	7	8	9	10
1	040480	14.9	N27W34	15.1	N07W(140)	840	15.7	17.9	8.0E+0
2	070680	01.3	N13W70				01.5	02.5	1.1E+1
3	070680	03.2	N14W70				03.4	04.0	1.0E+2
4	230381	06.8	N10W54	06.8	N30W(40)	400	07.0	08.5	2.2E+0
5	250381	20.7	N09W87	20.8	N25W(70)	900	21.2	24.7	1.3E+0
6	300381	00.0	N13W72	00.8	N10W(180)	1300	00.5	02.0	4.0E+0
7	040481	05.0	S44W87	04.7	S45W(35)	900	06.0	09.0	7.8E+0
8	280481	20.6	N16W90	21.0	N05W(30)	1000	21.5	25.1	4.0E+3
9	071181	03.9	S10W39				04.3	05.2	5.4E+0
10	141181	21.9	N16W49	21.5	N05W(110)	585	23.0	26.5	5.8E-1
11	051281	13.5	N20W40	13.4	N45W(60)	840	14.5	20.0	3.0E+0
12	020182	06.2	N19W88	05.8	N10W(40)	650	06.4	09.5	1.0E+1
13	080282	12.8	S13W88	12.8	N05W(10)	1310	13.0	14.1	1.0E+2
14	090282	04.0	S14W90	04.6	N05W(30)	1600	04.2	05.8	1.6E+2
15	070382	02.8	N19W53	03.0	N10W(60)	1140	03.3	05.7	7.0E+0
16	190782	00.7	N21W45	00.4	N45W(40)	630	01.0	02.5	6.0E+0
17	080882	02.0	S09W65	02.4	S10W(10)	600	02.2	05.0	6.0E-1
18	130882	22.9	N11W59	22.4	S30W(20)	300	23.0	23.7	3.2E+0
19	140882	05.0	N11W63				05.1	06.0	1.6E+2
20	221182	12.4	S08W34				12.7	14.0	8.0E+0
21	221182	17.6	S11W36	17.6	S10W(60)	740	18.0	20.7	3.0E+1
22	071282	23.6	S19W86	24.0	S10W(20)	1250	24.0	27.0	4.0E+2
23	050183	13.3	>W90				13.7	15.0	4.0E+1
24	150583	08.7	S10W80	08.9	S25W(50)	1110	09.0	11.2	5.0E+1

Here "1" is event number; "2"- event date; "3"- flare onset time, hrs, UT; "4"- flare location; "5"- CME limb time, hrs, UT; "6"- CME initial position angle and width (in parenthesies); "7"- CME velocity, km/s; "8"- electron event onset time, hrs,UT; "9"- time to maximum of >0.22 MeV electron intensity, hrs,UT; "10"- peak intensity of >0.22 MeV electrons, part/(cm**2*s*sr).

Table 5

Time and amplitude characteristics of ISEE-3 >0.22 MeV electron events and corresponding CME and Xt burst parameters

1	2	3	4	5	6	7	8	9	11	12
1	840	FPR	3.0	0.25	2.1	0.25	8.0E+0	5.0E-2	L	+
2	0	FPR	1.2	0.15	1.0	0.15	1.1E+1	2.0E-3	S	+
3	0	FPR	0.8	0.25	0.6	0.25	1.0E+2	7.0E-3	S	+
4	420	FPR	1.7	0.50	1.0	0.25	2.2E+0	8.5E-3	S	+
5	900	W50	2.5	0.75	2.0	0.50	4.7E+0	2.2E-2	S	+
6	1300	FPR	2.0	0.50	1.0	0.25	4.0E+0	3.5E-3	L	+
7	900	W40	3.6	0.50	2.5	0.25	1.2E+1	8.0E-3	S	-
8	1000	W48	3.2	0.50	3.0	0.50	1.2E+2	2.0E-2	L	+
9	0	FPR	1.3	0.25	0.8	0.25	5.4E+0	6.6E-3	S	+
10	615	FPR	4.6	0.50	4.5	0.50	8.0E-1	5.2E-3	L	+
11	905	FPR	6.5	0.75	5.5	0.75	3.2E+0	4.0E-4	L	-
12	650	W45	2.0	0.50	1.0	0.25	2.0E+1	7.0E-3	S	+
13	1310	FPR	1.3	0.25	1.1	0.25	6.0E+1	1.0E-2	S	+
14	1600	W33	1.5	0.25	1.6	0.25	2.0E+1	1.2E-2	S	+
15	1240	FPR	2.9	0.25	2.4	0.25	7.0E+0	2.7E-2	L	+
16	700	FPR	1.8	0.25	1.5	0.25	6.0E+0	1.0E-2	S	+
17	640	FPR	3.0	0.50	2.0	0.25	6.0E-1	7.0E-3	S	+

18	330	FPR	0.8	0.15	0.6	0.15	3.0E+0		S	+
19	0	FPR	1.0	0.15	0.7	0.15	1.6E+2		S	+
20	0	FPR	1.6	0.25	1.3	0.25	6.0E+0	2.0E-3	S	+
21	805	FPR	3.1	0.25	2.7	0.25	2.2E+1	7.3E-3	L	+
22	1250	FPR	3.4	0.25	2.5	0.25	5.0E+2	3.0E-2	L	+
23	0	FPR	1.7	0.50	1.0	0.25	6.0E+1		S	+
24	1110	FPR	2.5	0.25	1.0	0.25	1.0E+1	2.0E-2	S	+

Here "1" is event number (the same as in table 2); "2"- CME velocity,corrected according to (7), km/s; "3"- angular distance between observer's magnetic footpoint and flare location (FPR means that observation point is projected to fast propagation region in solar corona); "4"- time to maximum of electron event corrected accoding to (3),hrs; "5"- delta time to maximum, hrs; "6"- electron event rise time, hrs; "7"- delta electron event rise time, hrs; "8"- normalized peak intensity according to (5); "9"- peak intensity of soft X-ray event, part/(cm**2*s); "10"- soft X-rays duration (L-long, >1 hour, S-short, < 1 hour); "11"- Xh association.
In Fig.6 we present time to maximum (a) and rise time (b) vs corrected Vcme. Events NN 13,14 and 18 of Tables 4 and 5 were excluded from the figure as the corresponding flares were in opposite hemispheres with observed CMEs. Two doubhtful points with highest values of tm and trise concern NN 10 and 11 events. It seems these events are related to disturbances which were caused by filament dissapearance. We see from Fig.6 that tm and trise are slowly increasing with increasing Vcme and that all values of tm and trise are less for non-CME associated flares than for CME-associated ones. Open circles are for L, dark points - for S events. As there is no difference between L and S events in Fig.6 one may conclude that tm and trise are caused rather by time extended shock acceleration than by flare duration.

6. Phobos data and results

From July 1988 until March 1989, more than fifty solar energetic particle events were registered by the Low Energy Telescope (LET) onboard Phobos-2 s/c. The time period corresponds to the rising phase of solar cycle 22 when large number of flares and CMEs, followed by interplanetary shocks and SEP events occured.

The flux of electrons was measured by LET in the energy interval of 0.35-1.5 MeV with time resolution of 20 min. in angle from +60 to -115 deg relative to the Sun-s/c line. We also used solar wind and interplanetary magnetic feald data provided by TAUS [Logachev et al, 1995] and FGMM [Roatsch et al, 1989] experiments onboard Phobos-2, respectively. The time interval analysed covers both cruis phase and the Martian orbit phase of the mission.
Sharp intensity rise, followed by more or less gradual decay of the electron flux was considered as SEP event. Those enhancements having duration more than 2 hours and amplitude exceeding a background by 5 sigma were taken into account, corresponding to flux at maximum greater than 0.1 particle/(cm**2*s*ster). We selected 57 such electron enhancements. The list of these events is presented in Table 6.

Table 6

Phobos-2 SEP event characteristics and corresponding Xt bursts and CME parameters

1	2	3	4	5	6	7	8	9	10	11	12
1	0809	1850	1.3	1.0	4.8E2	7.0E2	0.2	1.2	1.2E-2	S	-
2	2709	0241	1.7	1.7	1.1E2	3.7E2	0.4	1.1	5.0E-3	L	-
3	2709	0640	1.2	1.6	6.0E1	3.2E2	0.3	1.1	4.7E-3	S	-
4	2709	0950	0.7	3.5	4.5E1	2.3E3	0.7	1.2	1.6E-2	L	Q→

5	2709	1607	5.2	7.6	4.5E2	2.3E4	1.0	1.1	7.9E-2	L	794
6	2809	2232	5.8	8.3	1.6E2	6.8E3	0.9	0.9	5.7E-2	L	800
7	3009	1900	5.1	3.3	5.0E1	9.4E2	0.8	1.1	1.7E-2	L	Q
8	0110	0723	2.2	1.7	6.0E2	1.0E3	0.2	1.0	1.8E-2	S	413
9	1010	1809	4.8	3.2	6.5E2	1.2E3	0.5	1.2	2.7E-2	L	+
10	1310	2030	3.6	3.2	2.7E3	5.4E3	0.5	1.0	6.4E-2	L	913
11	2111	2250	2.4	1.8	4.0E2	1.0E3	0.3	1.0	1.6E-2	S	315
12	0712	2333	1.7	2.3	1.4E1	1.6E2	0.4	1.2	1.0E-2	S	Q
13	0812	1956	0.7	2.5	4.0E1	5.0E2	0.4	1.2	5.3E-3	S	Q
14	0912	0316	0.0	0.0	4.0E1	1.2E3	1.0	1.0	2.2E-2	S	Q
15	0912	2117	7.6	7.4	1.0E2	2.1E3	1.1	0.8	2.6E-2	S	Q
16	1012	0453	2.5	3.2	5.0E1	6.4E2	0.9	0.9	9.4E-3	S	Q
17	1012	1426	9.6	7.0	1.4E2	1.6E3	1.1	1.2	2.2E-2	L	Q
18	1312	0130	0.8	3.1	1.7E2	1.5E3	0.5	1.0	2.0E-2	S	281
19	1312	1029	2.4	2.0	3.2E2	9.3E2	0.4	1.1	7.6E-3	S	-
20	1312	1405	1.9	1.9	1.0E2	5.0E2	0.4	1.1	6.5E-3	S	-
21	1512	0448	6.4	6.6	3.0E3	4.5E1	1.0	1.0	1.1E-1	L	Q
22	1612	0826	8.2	8.5	3.5E4	3.7E5	1.0	1.0	4.7E-1	L	+
23	1712	0343	4.7	2.1	2.0E3	7.8E3	0.7	1.1	2.8E-2	S	Q
24	1812	1651	5.8	5.5	1.8E3	1.1E4	0.9	1.0	1.1E-1	L	Q
25	2012	1218	4.2	3.8	3.7E3	3.3E4	1.0	1.1	7.3E-2	L	Q
26	2112	1553	4.1	4.1	2.2E2	2.7E3	1.0	1.0	1.5E-2	S	Q
27	2212	2307	3.9	4.8	2.3E3	8.5E3	1.0	1.1	5.3E-2	L	350
28	2412	0201	2.6	2.6	2.1E3	2.0E4	0.5	1.1	2.9E-2	S	+
29	2712	0527	6.4	5.1	1.3E3	4.2E3	0.9	1.2	1.3E-2	S	900
30	2712	0747	5.8	4.3	7.0E2	2.2E3	0.9	1.2	1.9E-3	L	961
31	2812	0024	4.2	3.1	5.5E2	2.0E3	0.6	1.3	2.1E-2	L	421
32	2812	0825	3.0	3.0	7.0E2	5.5E3	0.6	1.3	1.2E-2	S	Q
33	2812	2342	1.9	2.0	7.0E2	4.4E3	0.6	0.9	3.6E-2	S	376
34	0401	1807	2.8	2.0	4.5E3	1.5E4	0.6	0.8	4.7E-2	L	Q
35	1301	0932	2.5	1.9	4.5E2	2.0E3	0.5	1.1	2.3E-1	L	314
36	1301	1255	3.6	2.6	6.5E2	3.3E3	0.6	1.2	9.2E-2	L	Q
37	1801	0606	2.9	3.3	1.5E2	2.7E3	0.7	1.1	7.0E-2	L	725
38	1801	1804	1.4	0.9	8.0E2	3.0E3	0.3	1.1	9.6E-2	L	-
39	1901	0237	0.7	0.9	2.0E1	1.1E2	0.0	0.0	5.0E-3	L	-
40	0302	1408	2.2	3.7	1.2E2	6.5E2	0.8	1.1	3.0E-2	L	+
41	0702	0207	3.5	4.0	4.0E1	6.0E2	1.0	1.1	1.2E-2	S	-
42	0702	1443	2.0	2.5	1.0E2	1.1E3	0.6	1.0	9.0E-3	S	-
43	0702	1640	3.5	3.9	1.2E2	1.4E3	1.0	1.0	2.1E-2	S	-
44	0603	1354	4.1	5.7	7.0E4	2.7E6	1.1	1.2	1.5E0	L	+
45	0703	2236	4.4	5.1	3.3E3	9.7E4	0.9	1.0	4.2E-2	S	Q
46	0903	1000	1.3	1.8	1.3E4	1.5E5	0.7	0.7	7.6E-2	S	-
47	0903	1515	2.5	2.7	3.0E4	3.6E5	0.7	1.1	4.0E-1	L	+
48	1003	1109	4.5	4.4	2.0E3	1.6E4	1.0	1.1	4.5E-2	L	Q
49	1003	1842	7.8	7.2	1.2E5	1.2E6	1.0	1.3	4.5E-1	L	+
50	1103	0827	6.3	5.4	6.0E3	2.3E4	1.1	1.1	9.7E-2	S	Q
51	1103	1535	5.0	4.1	7.0E3	2.5E4	0.9	1.1	1.2E-1	S	Q
52	1103	1933	5.4	5.1	1.8E4	4.7E4	0.8	1.1	1.3E-1	S	Q
53	1203	0803	4.3	4.2	1.8E4	1.2E5	1.0	1.1	4.6E-2	S	Q
54	1703	1729	6.2	5.5	3.0E3	1.5E5	1.0	1.0	6.5E-1	L	698
55	1703	2310	3.3	5.0	7.5E2	3.6E4	1.0	1.1	2.4E-2	S	Q
56	2203	1949	4.4	3.4	9.5E1	5.9E2	0.9	1.0	1.0E-2	S	Q
57	2303	1925	1.3	2.6	2.4E4	4.2E5	0.5	1.1	1.5E-1	L	1400

Here 1 is event number; 2 - the date of an event; 3 - onset of H& flare (UT); 4 - peak intensity time from H& onset with subtracted coronal propagation time and normalized to 1 AU; 5 - rise time of electron profile normalized to 1 AU; 6 - peak intensity at the observation point; 7 - peak intensity, normalized to 1AU and to fast propagation region; 8-tau (see below), 9-q - fitting parameteres for time profile approximation; 10 - peak intensity of soft X-rays; 11 - soft X-ray duration (L-long, S-short, as in Table 5), 12 - CME association with measured (if it was) speed, Q - questionable.

We approximated Phobos time profiles by means of specially developed computer program "Fit". The approximating formula used is:

$$I(t) = Io*(D**3/B)*exp[-D/B**2], \qquad (11)$$

where D = tau/(t-to), B = 2-q.
All fitting parameters are obvious and discribed above.
We fitted the intensity time profile in the early phase of the event, i.e.around the time of maximum, where the effects of convection and corotation are small and the radial dependence of electron mean free path and subsequent interplanetary shocks are also less important.

Fig.7 shows examples of fits to electron intensity time profiles for three events, characterized by connection to parent flare. Upper curve demonstrates event with good connection to the FPR, middle and lower curves show examples of flare sites, located east and west from the magnetic footpoint, respectively. It can be seen from the figure that for all three events the rising phase is well described in the framework of diffusive propagation with q about 1 and assuming prompt injection at the flare onset time (marked on the figure by vertical dashed line) suggesting that electrons at the rising phase and around the maximum were accelerated in the impulsive phase of the flare. The fit is poor for eastern flare (middle panel) after the time of maximum flux, explainable by the effect of an interplanetary shock observed by Phobos-2 [Roatsch et al, 1989].

We approximated the intensity time profiles of all 57 SEPs similarly. The values of q were in the range of 0.8-1.3. The mean free path parallel to interplanetary magnetic field was 6*10**-2 - 4.5* 10**-1 AU which is close to the "consensus range" [Palmer, 1082] and to other experimental results [Kallenrode, 1993]. Results of fit show that q about 1, like for Helios profiles, is preferable to be used to normalize Imax and peak time to 1AU.

We have investigated the possible influence of coronal shocks on the parameters of SEP events. Out of the 57 LET events, we had firm information whether the parent flare was associated with CME for 33 events. In 15 cases the velocity of CME and its angular width were known. We looked at the variation of Imax and tm and obtained the tendency that they increase with increasing CME velocity. Scatter plot of tm vs. Vcme is given in fig.8 and cofirms the conclusion of Helios and ISEE 3 data analysis.

We have compared the normalized maximum electron flux Imax with the amplitude of soft X-ray bursts (Xt) for all 57 cases, the result is given in fig.9. Events belonging to long and short duration flares (29 and 28, respectively) are separated in the figure. The correlation coefficient between logImax and logXt is Rall = 0.85. Similar correlation was obtained for long and short duration events: Rs = 0.81 and Rl = 0.83, respectively. We have also calculated the correlation coefficient between logImax and the magnitude characterising the total energy released in 0.03-0.7 MeV X-ray bursts (log Xh), for 48 events, which was equal to 0.7.
Taking into account that Xt is proportional to the energy released in the flare and the total energy emiitted in Xh burst is the measure of the total number of the accelerated electrons, we may say that our result confirms the importance of impulsive flare acceleration as a source of energetic electrons in SEP events, despite of flare duration. This result does not support the idea that at long duration flares all the SEP electrons are accelerated by interplanetary shocks generated by the flare [Cane et al,1988, Moses et al, 1989].→

7. Conclusions

1. Calculations of time of intersection between CME-driven shock and observer`s magnetic field line on the basis of geometric consideration presented in Table 1 show that all calculated time intervals are considerably less than observed peak intensity times and thus, CMEs can contribute to particle flux at observation point. The exceptions are events NN 7 (far behind the east limb observer`s magnetic footpoint), 18, 30 and 31 (see remarks in the text), when calculated time of CME-driven shock arrival is higher than observed time to maximum. Moreover, Dec.5,1981 1982 event was connected not to flare but to disappearing filament. If it is right, then energetic electrons could be accelerated by CME-driven shock.
2. The dependencies of electron rise time and time to maximum vs. Vcme were studied. On average both tm and trise show a tendecy to increase with increasing CME speed. This can be a result of CME acceleration and followed deceleration in solar corona and thus prolonged ability to accelerate particles of ambient plasma above some minimal value of CME speed contrary to the case of constant speed.
3. The dependence tm vs. Vcme is more pronounced than in the case of trise. It means either acceleration due to CME begins near flare impulsive phase or our procedure of normalization must be applied to time of the first electron arrival to observation point.
4. The dependence of tm on Vcme is practically the same for CME associated both impulsive and long duration flares. This confirms possibility of electron acceleration by CME-driven shock.
5. On the other hand it was obtained that amplitudes of energetic electron fluxes in SEP events with and without CMEs are well correlated with amplitudes of Xt-bursts independent of birst duration. It means that flux amplitude of accelerated electrons is related to total energy realized in flare.
6. So according to pp.1-4, on the one hand, and p.5, on the other hand, we can say that energetic electron intensity profiles are explained in the framework of two sources or acceleration mechanisms: impulsive flare acceleration and CME-driven shock acceleration. Relative importance of these sources is determined in each case by concrete conditions but CME effect is more pronounced when CME velocity is large.
7. As a by product of this investigation it was obtained that interplanetary propagation of >0.3 MeV electrons may be described by radially dependent diffusion with diffusion coefficient proportional to r**q with q about of 1.

Further understanding of the problem may be obtained by investigation of energetic electron spectra and intensity anisotropy after flares with and without CMEs. Logical development of our approach is related with complex consideration of geometric, kinematic and dynamic parameters of CMEs and subsequent formation of coronal shock.

The results of Phobos data investigation were reported and published in the proceedings of 24 International Cosmic Ray Conference. The results of analysis of Helios data were reported on the "Second Volga International Summer School on Space Plasma Physics". The report will be published in the russian journal of "Radiofizika" ("Radiophysics and Quantum Electronics"- transl.). Some aspects of our approach are presented to Russian conference on Solar Physics (Moscow, Dec. 6-8, 1995).
Detailled paper for "Astrophisical Journal" or "Solar Physics" is on preparation now. →

Acknowledgements.

We are grateful to I.Richardson from Laboratory of High Energy Astrophysics, GSFC, for ISEE 3 energetic electron profiles, N.R.Sheeley from Naval Research Laboratory for CME list according to Solwind coronograph measurements and Mrs. J.T.Burkepile from High Altitude Observatory, Boulder for "Catalogue of Mass Ejections Observed by the SMM Coronograph". We are also grateful to Dr. J.Feynmann for helpful discussions.
We are extremely grateful to Dr. S.Kahler from Phil.Lab. who was the initiator of this investigation.
We thank EOARD AF for this contract.

Stolpovskii Daibog

REFERENCES

W.I.Axford, 1981, Proc. 17 ICRC, 12, 155.
R.D.Blandford, 1994, Ap.J., Suppl.Series, 90, 515.
R.D.Blandford, Ostriker,1978, Ap.J.,221, L29.
H.V.Cane, 1995, Nucl.Phys. (Proc. Suppl.), 39A,35.
H.W.Cane, S.W.Kahler, N.R.Sheeley Jr., 1986, JGR, 91,13,321.
H.V.Cane, D.V.Reams, T.Von Rosenving, 1988, JGR, 93, 9555.
E.W.Cliver, S.W.Kahler, P.S.McIntosh, 1983, Ap.J.,264,699.
E.W.Cliver, S.W.Kahler, M.A.Shea, D.F.Smart, 1982, Ap.J., 260, 362.
E.I.Daibog, V.G.Stolpovskii, V.F.Melnikov, T.S.Podstrigatch, 1989, Astronomical Journal Let. (rus.), 15, 951.
E.I.Daibog, V.G.Kurt, Yu.I.Logachev, V.G.Stolpovskii, 1989, Kosm. Issled., 27, 113.
R.B.Decker, 1983, JGR, 88,9959.
D.C.Ellison, R.Ramaty,1985, Ap.J., 298, 400.
P.A.Evenson, P.Meyer,, S. Yanagita, 1982, JGR, 87, 625.
J.T.Gosling,1993, JGR, 98, 18,937.
A.J.Hundhausen, 1993, JGR, 98, 13,177.
A.J.Hundhausen, J.T.Burkepile, O.C.St.Cyr, 1994, JGR, 99, 8451.
S.W.Kahler, 1984, Solar Phys., 90,133.
S.W.Kahler, N.R.Sheeley,Jr.,M.Ligget, 1989, Ap.J.,344, 1026.
S.W.Kahler, 1994,Ap.J.,428,837.
S.W.Kahler, E.I.Daibog, V.G.Kurt, V.G.Stolpovskii, 1994, Ap.J., 422, 394.
S.W.Kahler, V.G.Stolpovskii, E.I.Daibog, 1994, Proc.,IAU Colloq.144, 479.
M.-B.Kallenrode, private communication
M.-B.Kallenrode, G.Wibberenz, 1991, Ap.J., 376, 787.
G.F.Krymskii, S.I.Petuchov, 1980, Soviet Astr. Letters, 6, 124.
H.Kunow, G.Wibberenz, et al, in Physics of Inner Heliosphere, (R.Shwenn,E.Marsch,eds), p.II, 1991, Springer-Werlag, p.243.
M.A.Lee,1982,JGR,87,5063.
M.A.Lee,J.M.Ryan,1986, Ap.J.,303,829
R.P.Lin, 1985, Sol.Phys., 100, 537.
R.P.Lin, H.S.Hudson, 1971, Sol.Phys., 17,412.
R.P.Lin, R.A.Mewaldt, M.A.L.Van Hollebeke, 1982
Yu.I.Logachev, V.G.Stolpovskii, E.I.Daibog, et al, Izvestija RAN, ser. fiz, 1995, 59, 41.
J.D.Palmer, 1982, Rev.Geophys.Space Phys., 25, 335.
V.L.Prischep, V.S.Ptuskin, 1981, Soviet Astr., 25, 446.
U.R.Rao, K.G.McCraken, R.K.Bukata, 1967, JGR, 72, 4325.
T.Roatsch et al, 1989, "Phobos-2 FGMM Data during Cruise, IKF Preprint 8/89, Berlin.
N.R.Sheeley,Jr., private communication.
N.R.Sheeley,Jr. et al. 1985, JGR, 90, 163.
R.B.Tsurutani, R.P.Lin, 1985, JGR, 88, 5645.
M.A.I.Van Hollebeke, L.S.Ma Sung, F.B.McDonald, 1975, Solar Phys., 41, 189.
R.Woo, J.W.Armstrong, et al, 1985, JGR, 90,154. →

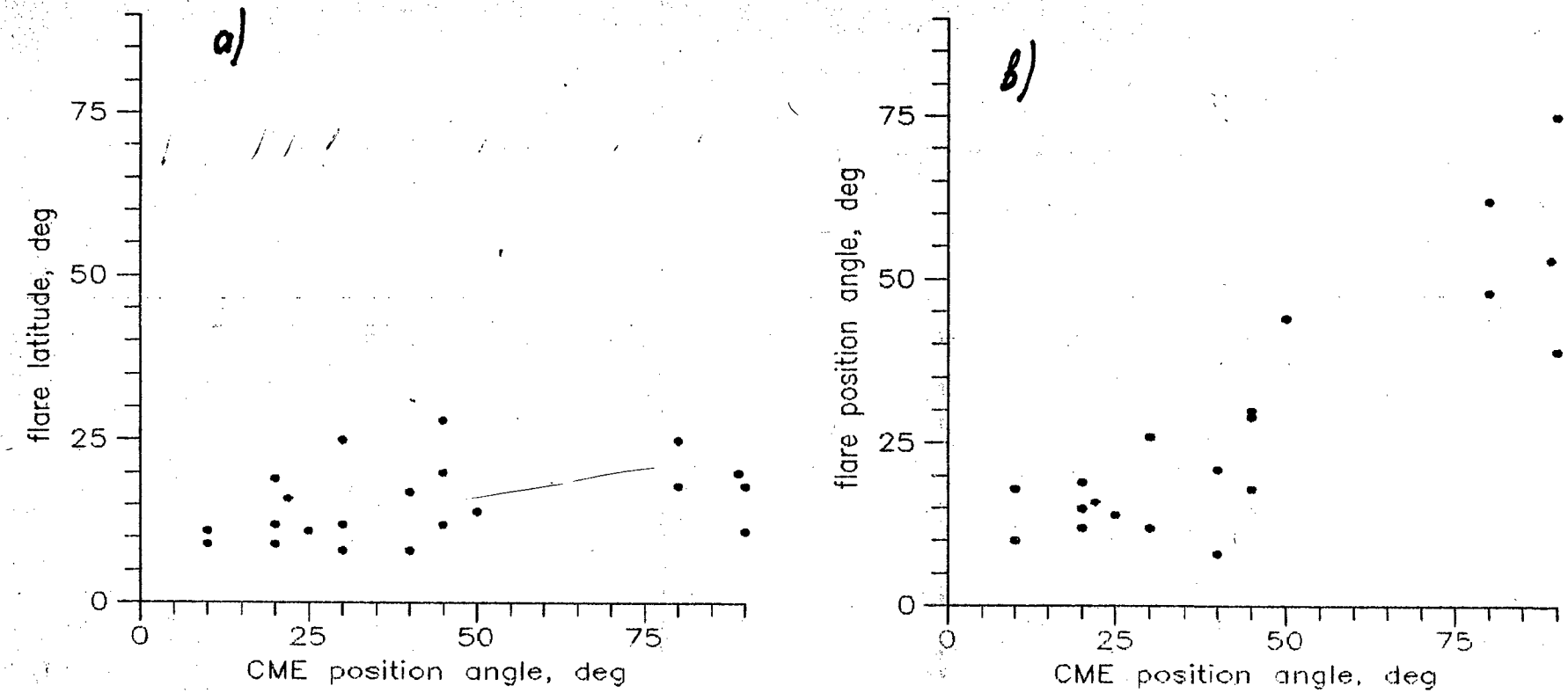
a)
flare latitude, deg
0
25
50
75
0
25
50
75
CME position angle, deg
b)
flare position angle, deg
0
25
50
75
0
25
50
75
CME position angle, deg

Fig. 1

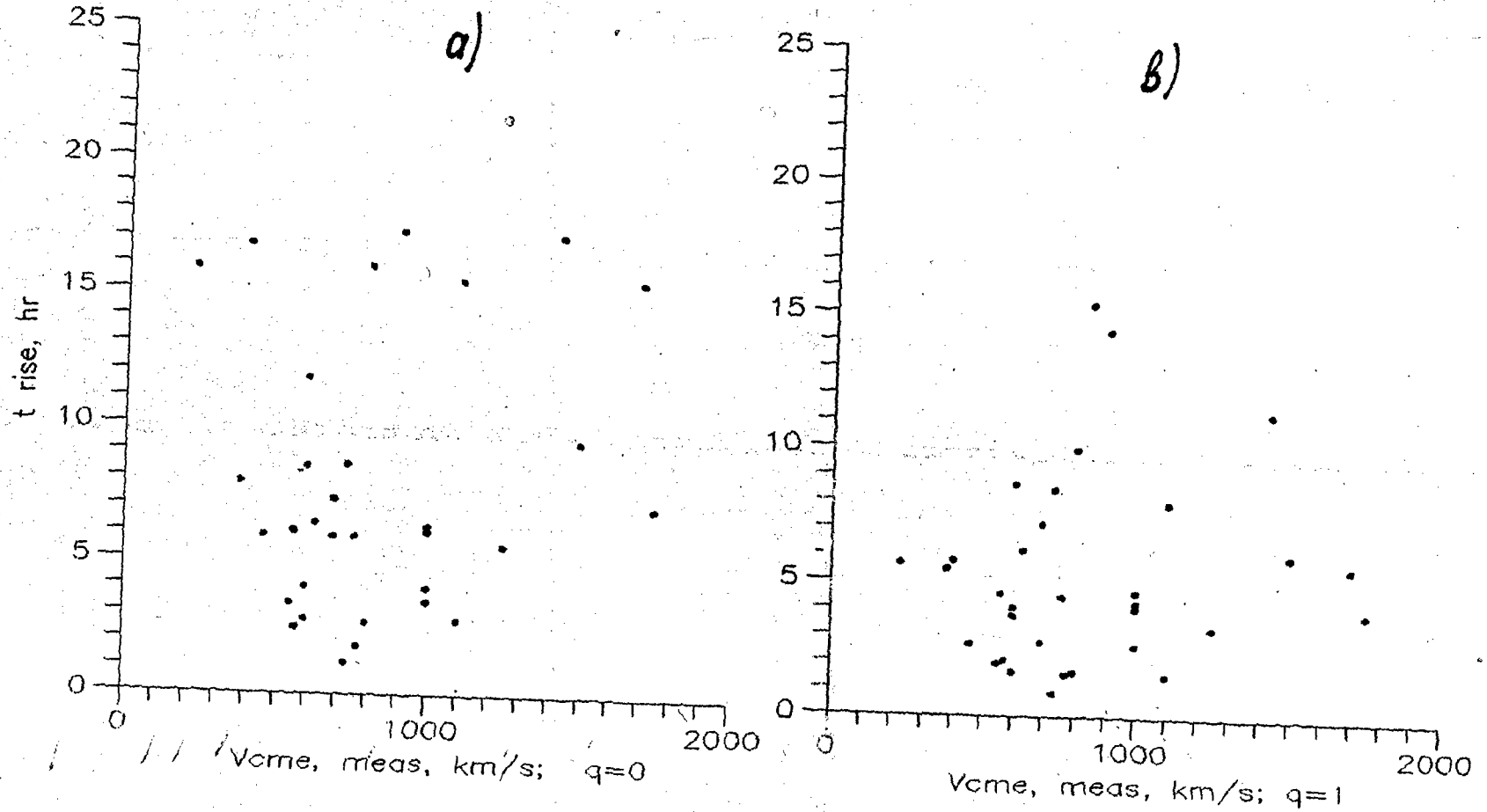
a)
b)
t rise, hr
25
20
15
10
5
0
0
1000
2000
Vcme, meas, km/s; q=0
Vcme, meas, km/s; q=1

Fig.2

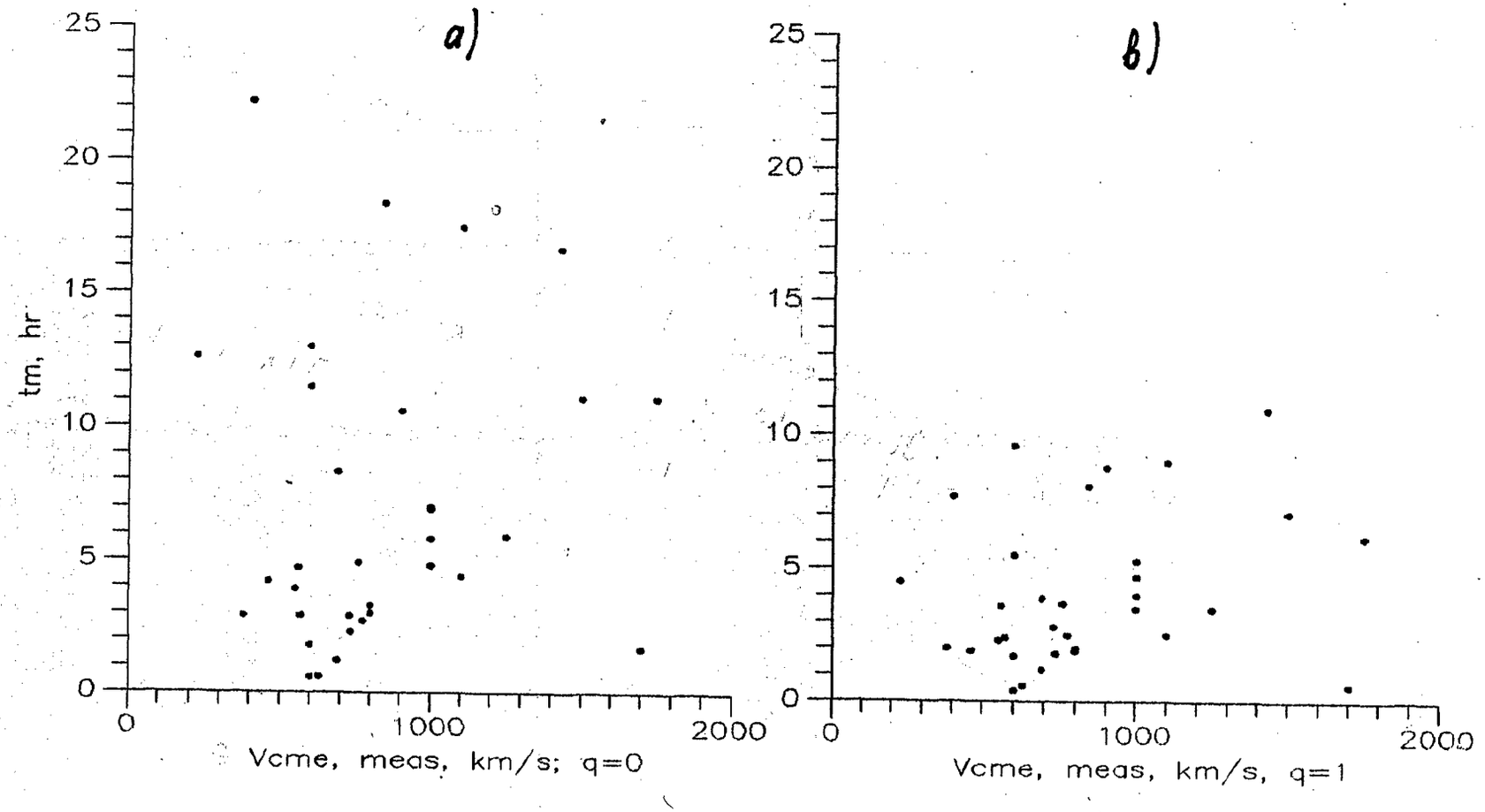
a)
b)
25
20
15
10
5
0
tm, hr
0
1000
2000
Vcme, meas, km/s; q=0
Vcme, meas, km/s, q=1

Fig. 3

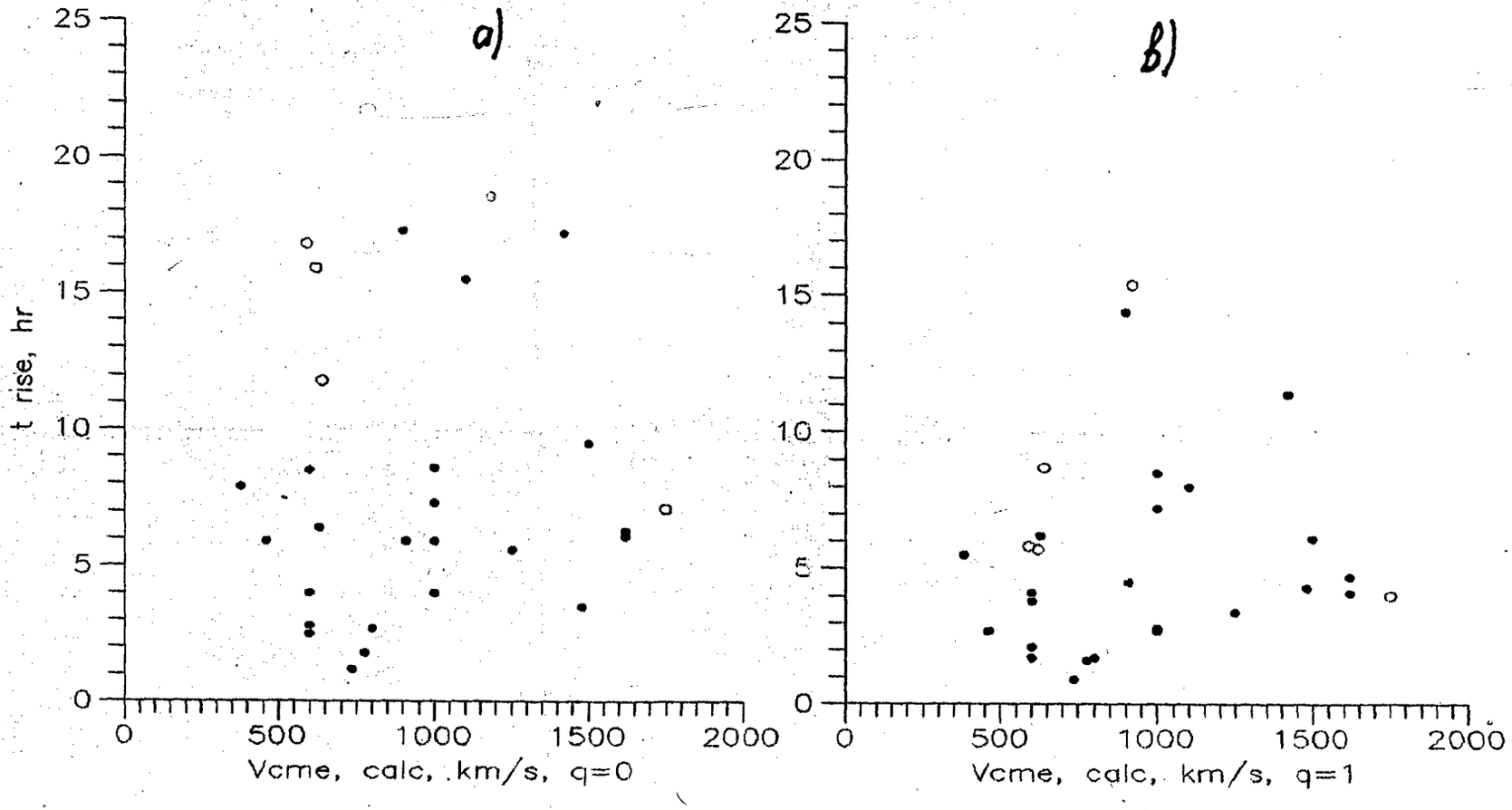
a)
b)
t rise, hr
0
5
10
15
20
25
0
500
1000
1500
2000
Vcme, calc, km/s, q=0
Vcme, calc, km/s, q=1

Fig. 4

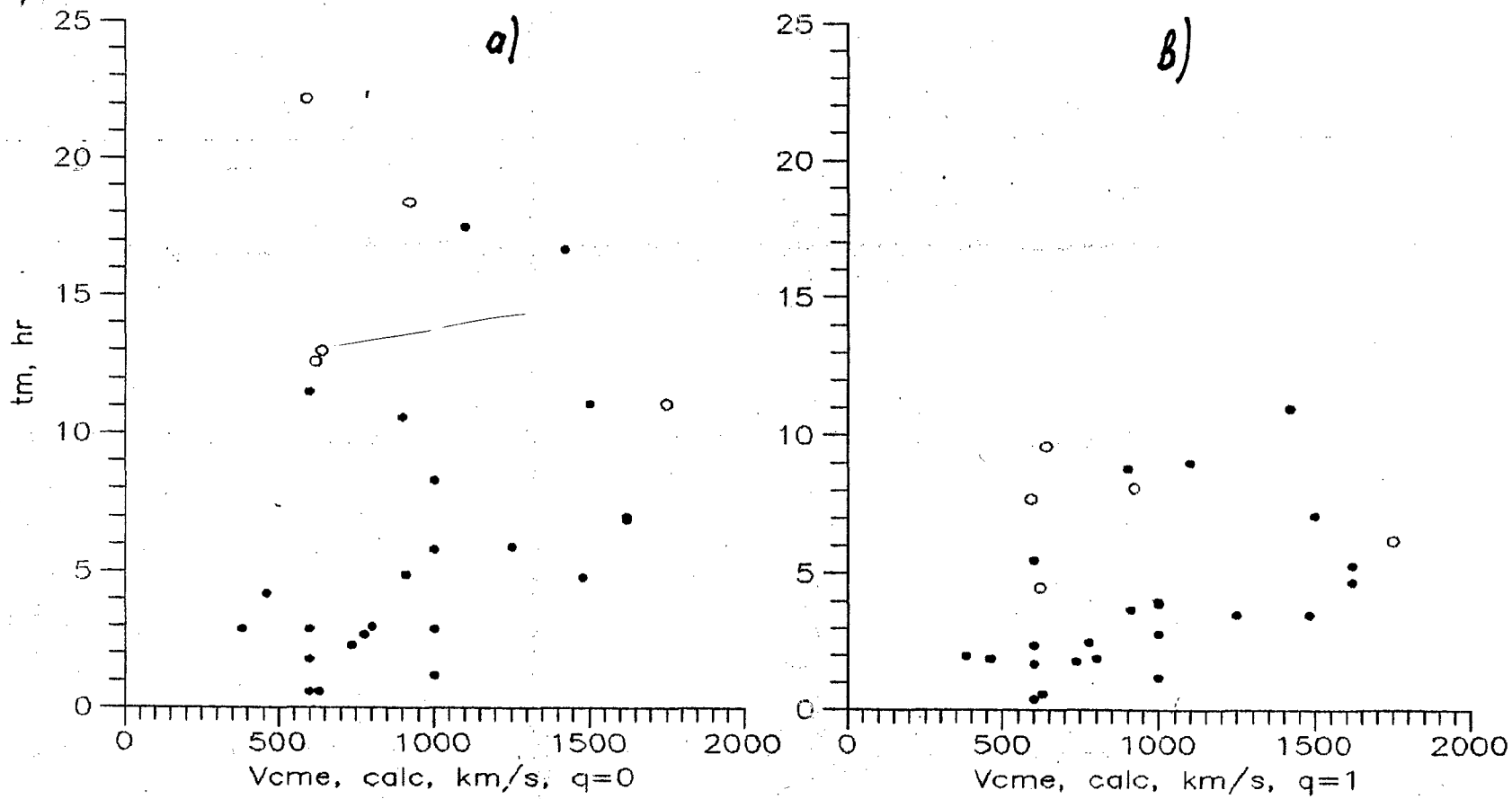
a)
b)
tm, hr
25
20
15
10
5
0
0
500
1000
1500
2000
Vcme, calc, km/s, q=0
Vcme, calc, km/s, q=1

Fig. 5

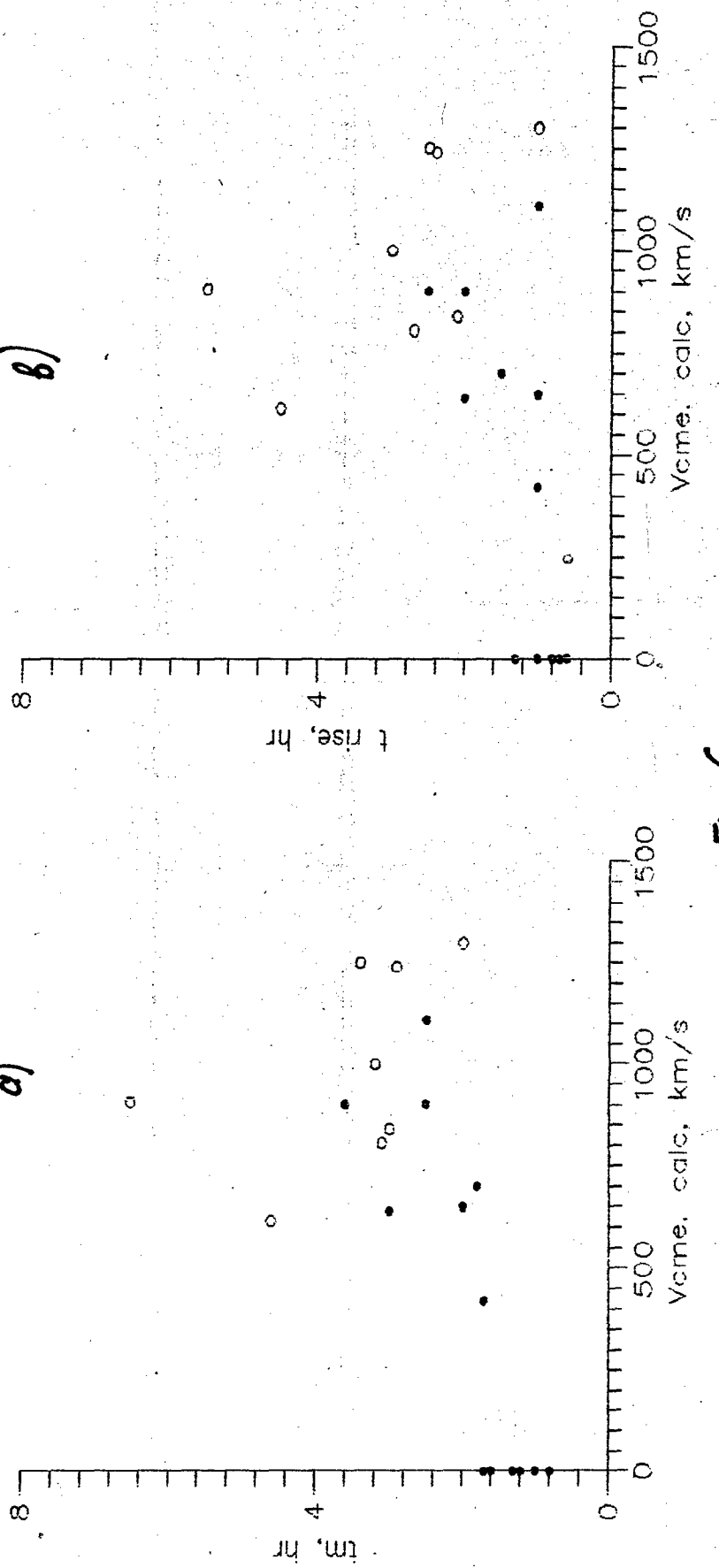

Fig. 6

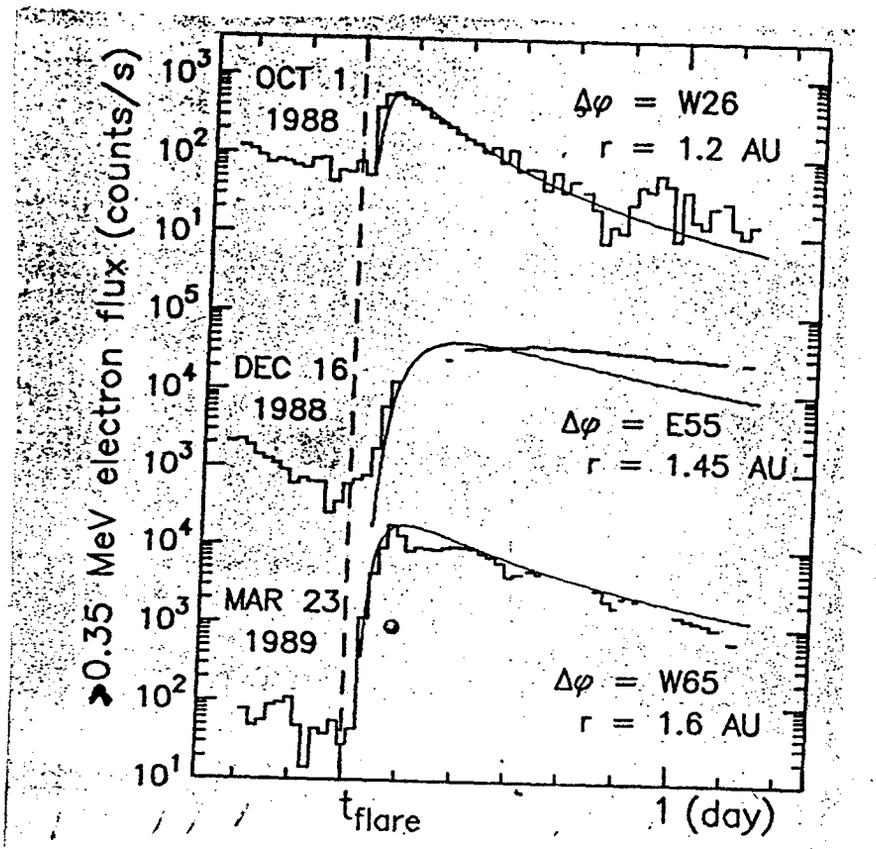

Figure 7. *Examples of fits to electron flare events*

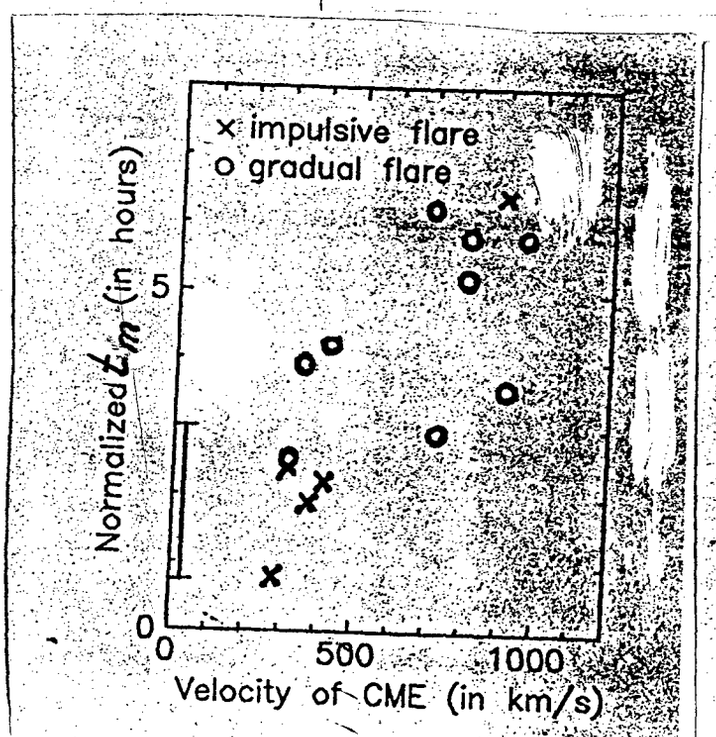

Figure 8. *Normalized time to maximum intensity, as a function of CME velocity*

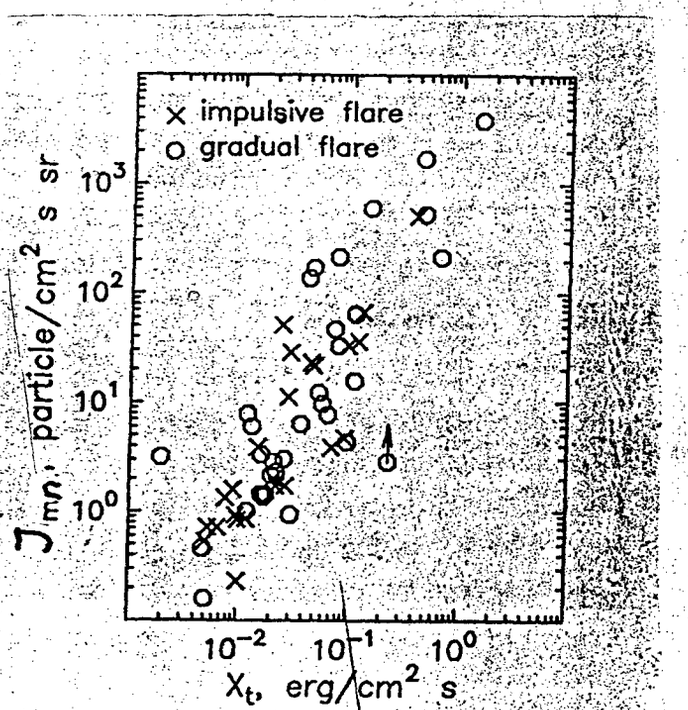

Figure 9. *Normalized >0.35 MeV electron flux at SEP event maximum, as a function of the amplitude of soft X-ray burst*